



**Universiteit
Leiden**
The Netherlands

Towards peptide based therapeutics-applications in celiac disease and infectious diseases

Kapoerchan, V.V.

Citation

Kapoerchan, V. V. (2009, December 22). *Towards peptide based therapeutics-applications in celiac disease and infectious diseases*. Retrieved from <https://hdl.handle.net/1887/14542>

Version: Corrected Publisher's Version

License: [Licence agreement concerning inclusion of doctoral thesis in the Institutional Repository of the University of Leiden](#)

Downloaded from: <https://hdl.handle.net/1887/14542>

Note: To cite this publication please use the final published version (if applicable).

Chapter 6

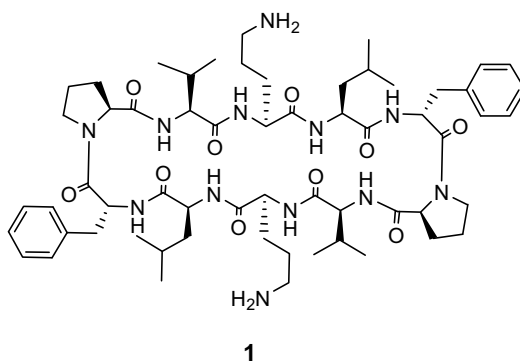
Turn-Modified Gramicidin S Analogs Containing Morpholine Amino Acids

Submitted for publication:

Kapoerchan, V. V.; Spalburg, E.; De Neeling, A. J.; Mars-Groenendijk, R. H.; Noort, D.; Otero, J. M.; Ferraces-Casais, P.; Llamas-Saiz, A. L.; Van Raaij, M. J.; Van Doorn, J.; Van der Marel, G. A.; Overkleef, H. S.; Overhand, M. 'Gramicidin S derivatives containing cis- and trans Morpholine Amino Acids (MAAs) as turn mimetics' Chem. Eur. J.

Introduction

The cyclic decapeptide Gramicidin S (GS, **1**, *cyclo*-(Pro-Val-Orn-Leu-^DPhe)₂, Figure 1), produced by *Bacillus Brevis*,¹ displays efficient antibacterial activity against both Gram-positive and Gram-negative bacteria.² GS kills bacteria by disrupting the bacterial cell membrane,³ and this is attributed⁴ to both the basic and amphiphilic nature of its rigid cyclic β -hairpin molecular structure.⁵ This structure is stabilized by four intramolecular H-bonding interactions formed between the carbonyl and amine functionalities of the amides of opposing Val and Leu residues and by the two-residue turns of the ^DPhe-Pro sequences. The side chains of the two Orn residues are on one side of the molecule and the hydrophobic side chains of the two Val and Leu residues reside on the opposing face, making the molecule amphiphilic. GS also lyses human red blood cells, which limits its use to the treatment of topical infections.⁶ The fact that GS and similar cationic peptides do not target a specific bacterial gene product implies that antibiotic resistance against this type of compounds does not readily occur.⁷ Thus, GS analogs with an improved biological profile are interesting leads for the development of efficient broad-spectrum antibiotics.

Figure 1 The structural formula of GS.

Because of its well-defined secondary structure, GS has served as a model to probe the effect of turn-mimetics on the cyclic β -hairpin structure. The $^{\text{D}}\text{Phe-Pro}$ sequence of GS has been replaced with bicyclic thioindolizine derivatives⁸ as well as the structurally related 5,6-fused azabicycloalkanes⁹ and indolizines.¹⁰ In a related approach, several sugar amino acids (SAA) have been incorporated and their structural and biological properties were studied.¹¹ C-functionalized morpholines are found frequently both in natural products and in drugs.¹² Various synthetic strategies towards these compounds have been developed, making it possible to obtain morpholines with different substitution patterns. Because of its rigid structure, a morpholine ring incorporated in a GS molecule could possibly invoke structural changes which may have an influence on the antibacterial and hemolytic properties. This Chapter describes the synthesis of four GS analogs in which one of the $^{\text{D}}\text{Phe-Pro}$ turn motifs is replaced with a morpholine amino acid (MAA), and the evaluation of their structural and biological properties.

Design and synthesis of the target compounds

Previously, the synthesis of MAAs **2**, **3** and **4** (Figure 2) was described.¹³ These amino acids were readily accessible from the commercially available carbohydrates D-mannitol, D-ribose and D-glucosamine, respectively. MAA **5** (Figure 2) has not been reported before and the synthesis thereof is described here.

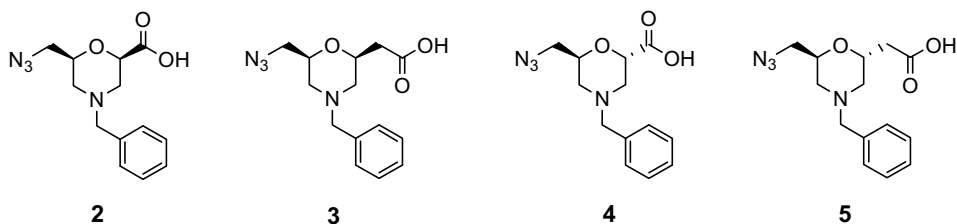
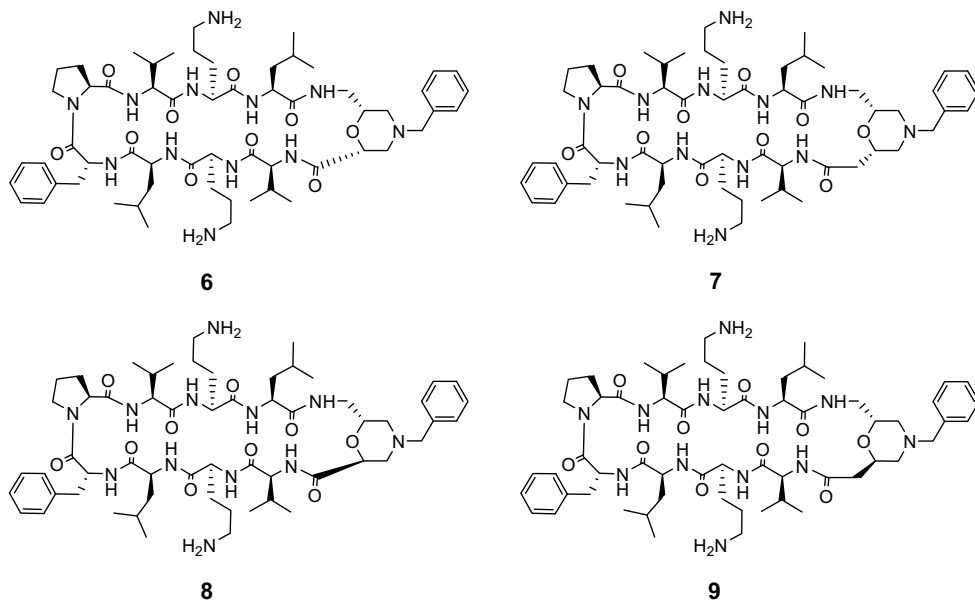
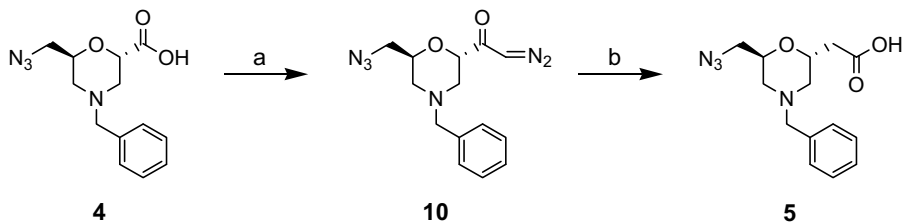
Figure 2 MAA's used for incorporation in GS.

Figure 3 GS analogs containing morpholine amino acids.

Amino acids **2** and **4** represent dipeptide isosteres and amino acids **3** and **5** are one carbon atom longer. Furthermore, the difference between **2** and **3** on one hand and **4** and **5** on the other hand, lies in the spatial relationship between the azidomethyl- and carboxyl groups (*cis* and *trans*, respectively). Incorporation of MAA's **2-5** would lead to GS analogs **6-9**, respectively (Figure 3), of which **7** has been synthesized before, but not evaluated for its structural and biological properties.¹³

MAA **5** was prepared by an Arndt-Eistert homologation of amino acid **4** (Scheme 1).¹⁴

Scheme 1 The synthesis of MAA **5** using an Arndt-Eistert homologation.

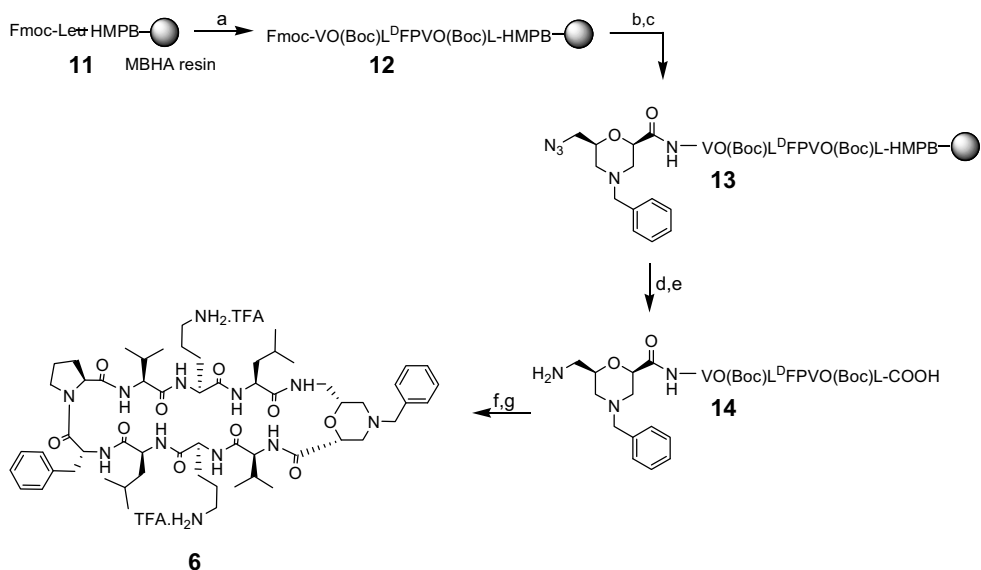
Reagents and conditions: a) i. EtCOCl, Et₃N, THF, -15 °C, 15 min. ii. CH₂N₂, 0 °C to rt, 3 h, 53%. b) CF₃COOAg, Et₃N, THF/H₂O 10:1, -25 °C to rt, 26 h, 33%.

After *in situ* preparation of the asymmetric anhydride of **4**, addition of diazomethane yielded diazoketone **10**. The use of diazomethane was necessary because the safer alternative (trimethylsilyl)diazomethane did not give productive diazoketone

formation. Subsequently, the formed diazoketone **10** was subjected to a Wolff rearrangement employing silver trifluoroacetate and base, to give **5** in 33% yield.

GS analogs **6-9** were synthesized using standard Fmoc SPPS methods and an example is given in Scheme 2. Starting from preloaded resin **11**, the peptide was elongated using commercially available Fmoc-amino acids. After attachment of MAA **2** as final amino acid, the azide functionality was reduced using PMe_3 and the peptide cleaved from the resin. Cyclization under the agency of PyBOP, HOBt and DIPEA, subsequent deprotection of the Boc protecting groups and purification were straightforward, yielding peptide **6** in a yield of 28%. Compounds **7**, **8** and **9** were synthesized in a similar fashion and the peptides were obtained as the TFA salts in 66% (**7**), 31% (**8**) and 52% (**9**) yield, respectively.

Scheme 2 Representative synthesis of **6** using standard Fmoc SPPS methods.



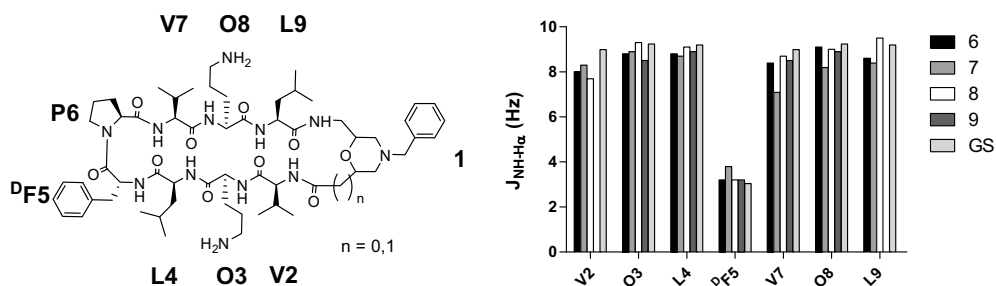
Reagents and conditions: a) repeated coupling cycles consisting of: i. Fmoc deprotection (20% piperidine/NMP, 15 min). ii. Amino acid condensation (3 eq Fmoc-AA-OH, 3 eq HCTU, 3.6 eq DIPEA, NMP, 2 h). b) Fmoc deprotection (20% piperidine/NMP, 15 min). c) 2 eq **2**, 3 eq PyBOP, 3 eq HOBt, 3.5 eq DIPEA, NMP, 16 h. d) 16 eq PMe_3 , dioxane/ H_2O 10:1, 6 h. e) 1% TFA/DCM, 4 x 10 min. f) 5 eq PyBOP, 5 eq HOBt, 15 eq DIPEA, DMF, 16h. g) 50% TFA/DCM, 30 min, 28% after HPLC purification.

Structural analysis of synthesized GS analogs

To evaluate their secondary structure, NMR spectra of analogs **6-9** were recorded at 298 K. All analogs assume a well-defined secondary structure in solution. In the amide region of the ^1H NMR spectra eight signals were seen for all analogs, as expected, because the analogs are not C2-symmetric like GS. However, some amide signals in

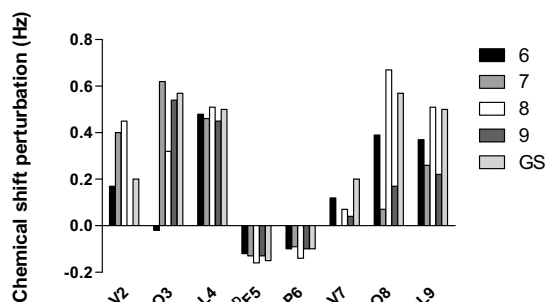
the ^1H spectrum of **9** were observed as broad singlets instead of doublets and the amide signal of the MAA residue was not observed at all, possibly indicating structural changes in the turn region of the molecule as compared to the natural product. To investigate the nature of these changes, further analysis was performed on the ^1H NMR data. The $J_{\text{NH-H}\alpha}$ values of all residues were compared to those of GS (Figure 4). The $J_{\text{NH-H}\alpha}$ coupling constants of the ornithine, leucine and valine residues were all between 8 and 12 Hz, which is a strong indication of a β -strand conformation.¹⁵ The $J_{\text{NH-H}\alpha}$ values of the D-phenylalanine residues were in the range of 2-4 Hz, which is typical for an amino acid as part of a β -turn.¹⁵ Therefore, except possibly for **9**, all analogs adopt a secondary structure highly similar to that of GS.

Figure 4 Comparison of $J_{\text{NH-H}\alpha}$ values of the analogs **6-9** to those of GS. In analog **9**, the amide signals of the V2 and L9 residues were observed as singlets, and therefore no coupling constant could be determined. The $J_{\text{NH-H}\alpha}$ values for analog **7** were taken from ref 13.



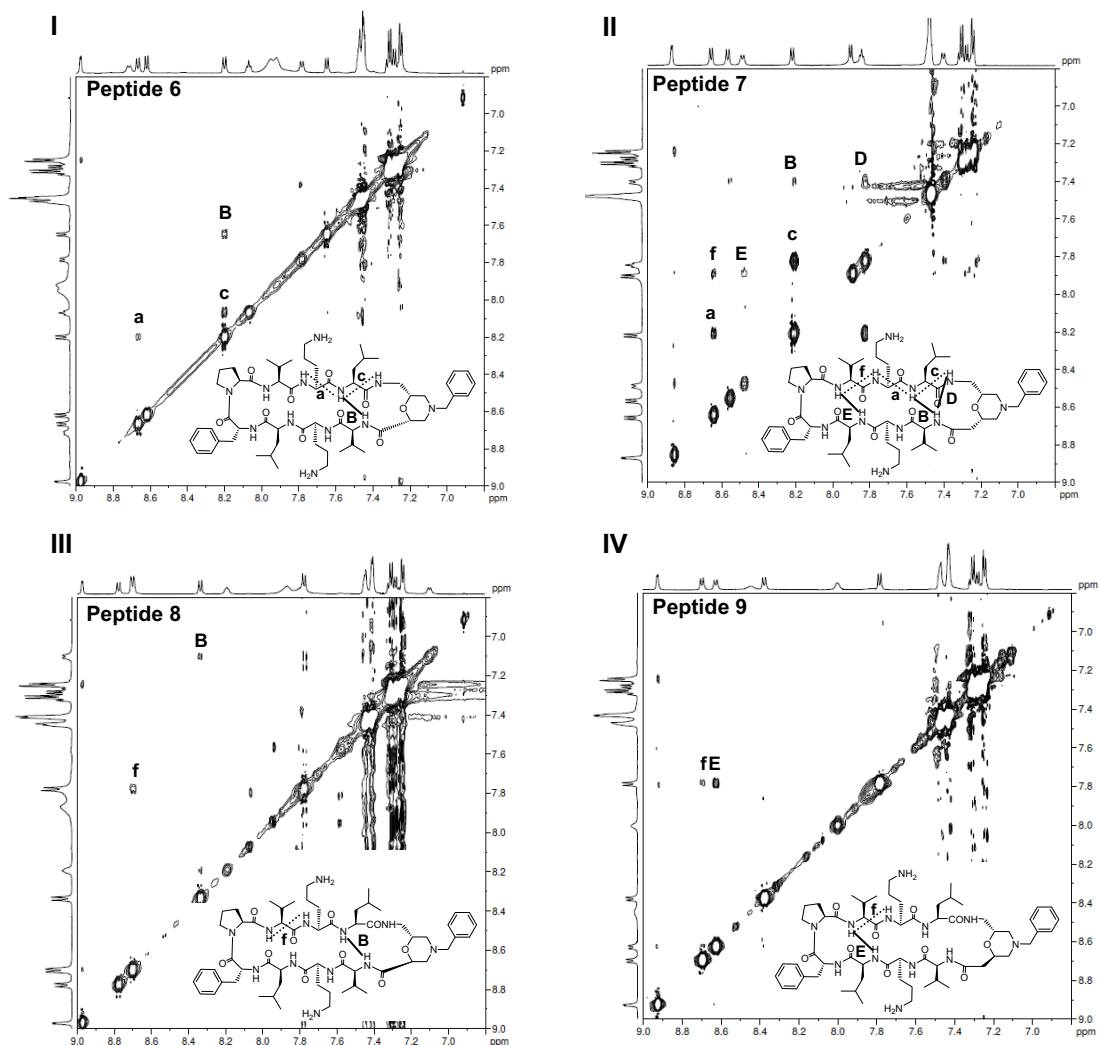
A different NMR analysis method was used to confirm the results described above (Figure 5). The chemical shift perturbation method¹⁶ compares the chemical shift of the α -proton of an amino acid residue to the average value of the α -proton of the same residue in a random coil conformation. Based on the (either positive or negative) differences seen, it can be determined whether the residue is part of a strand or turn region. As can be seen in Figure 5, almost all residues show the same perturbation signs as observed for GS. The valine, ornithine and leucine residues show positive perturbations indicating that these residues are part of a β -strand and all proline and D-phenylalanine residues display negative perturbations, indicating their presence in a turn. However, large differences in perturbation values are seen when the analogs are compared to GS. This might indicate that the β -sheet character of the analogs decreases.

Figure 5 Chemical shift perturbation of H_α protons in GS analogs **6-9** as compared to GS. For ornithine residues, the reported¹⁶ δ(H_α) random coil value of lysine was taken. The chemical shift perturbation was calculated as $\Delta \delta H_{\alpha} = \delta H_{\alpha}(\text{observed}) - \delta H_{\alpha}(\text{random coil})$. For the V2 residue of **9** no difference between the observed and reported value was observed. The H_α of V7 in **7** was not observed.



To obtain detailed molecular information nuclear Overhauser effect (NOE) experiments were performed for all analogs at 298 K. The amide NH regions of the compounds **6-9**, generally the most informative area for structural analysis of peptides, are depicted in Figure 6. For peptide **6**, a sequential NOE connectivity between the NH of Orn8 and the NH of Leu9 is observed (peak a, Figure 6, panel I, residue numbering as in Figure 4). Also, a long range NOE crosspeak between Val2 and Leu9 (peak B), and a sequential signal between the MAA residue and Leu9 (peak c) are observed. This means that these NH protons are close to each other. As such correlation signals are often found for GS itself, the presence of the same NOE crosspeaks in **6** points towards a conformation very similar to that of GS. Peptide **7** showed crosspeaks between Val2 and Leu9 (B, Figure 6, panel II), the MAA and Leu9 (c) and Orn8 and Leu9 (a), and three additional peaks are seen between MAA and Val2 (D), between Leu4 and Val7 (E), and between Val7 and Orn8 (f). Furthermore, while in panel I peaks B and c have roughly the same intensity, in panel II peak c has a much higher intensity than peak B. The NOE signals seen for peptide **7** generally point towards a GS-like conformation, however, the difference in intensity and the presence of an additional peak in the MAA-containing turn may indicate a slight distortion from the GS conformation. Compound **8** showed NOE crosspeaks between Val2 and Leu9 (B, Figure 6, panel III), as well as between Val7 and Orn8 (peak f), again indicating that its conformation does not differ much from that of GS. Peptide **9** showed crosspeaks between Val7 and Leu4 and Val7 and Orn8 (Figure 6, panel IV). Other crosspeaks were not observed, probably indicating that the turn containing the MAA was distorted.

Figure 6 Close-up of the NH-NH regions of ROESY spectra in CD₃OH at 298 K of compounds **6-9** (as depicted in panels I-IV) and the assigned correlations. Dashed lines and lowercase signals indicate sequential NOEs, solid lines and uppercase signals are long-range NOE signals.



An attempt was made to crystallize all analogs **6-9**, but only peptides **7** and **8** yielded crystals suitable for X-ray analysis. Peptide **7** shows a similar secondary structure in the crystal as GS, but the β -turn containing MAA **2** is distorted. As a consequence, only three instead of the usual four hydrogen bonds can be observed, due to the ‘flip’ of the amide bond connecting the MAA and the neighboring Leu residue (See appendix, Figure 7a). The distorted turn region is in agreement with the findings of the NMR experiments. Interestingly, this ‘amide flip’ has been observed previously for a GS analog in which one ^DPhe-Pro dipeptide was replaced with a sugar amino acid

(SAA).^{11a} The monomer of **8** shows a secondary structure similar to that of GS (See Appendix, Figure 7b). Comparison of the distance information with respect to the turn region of both GS and peptide **8** (Table 1) reveals that the determined distance between Val2-NH...O=Leu9 is more than 1 Å longer than the corresponding distance in GS and the N-H...O angle is too short (122.7° versus 161.5°). Whether this is considered a hydrogen bond is therefore disputable¹⁷ but fact is that the Val2-NH...O=Leu9 functionalities are rigidly positioned in close proximity in compound **8**. Therefore, in spite of the lack of an intramolecular hydrogen bond in the MAA-containing turn region of **8** the geometry of the two peptide bonds involved in the turn is quite similar to the usual β -turn motive in GS.

Table 1 Structural data extracted from the crystal structures of GS and **8**.

	GS ¹⁸	Peptide 8
Leu9 O ... H-N Val2	2.15 Å	3.31 Å
Leu9 O ... N Val2	2.99 Å	3.86 Å
Angle O ... H-N	161.5°	122.7°

Interestingly, peptide **8** forms a channel in the solid state (See Appendix, Figure 8a). This channel has a charged interior and a lipophilic exterior (See Appendix, Figure 8b). The MAA residues are outlined accordingly to the monomers, with the backbone carbonyl forming an intermolecular hydrogen bond to the α NH of an ornithine residue of the monomer next to it (See Appendix, Figure 8c). The supramolecular arrangement of **8** shows similarity to that of the same SAA-containing GS analog mentioned above which showed the ‘amide flip’ as well.^{11a} X-ray analysis showed that this particular GS analog formed a ‘ β -barrel’ structure consisting of six molecules which was stabilized by intermolecular hydrogen bonds and with the ornithine side chains pointing to the inside of the barrel. However, peptide **8** does show less ‘amide flip’ than the SAA-containing peptide and compound **7**.

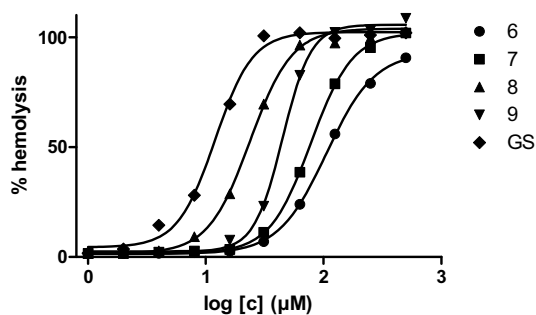
Evaluation of biological characteristics

GS analogs **6-9** were assayed against a panel of Gram-positive and Gram-negative bacterial strains. The results are shown in Table 2.

Table 2 The antibacterial activity of compounds **6-9**. MIC-values (MIC = Minimal Inhibitory Concentration) are given in $\mu\text{g}/\text{ml}$ and were measured after 24 hours of incubation.

	Gram+ <i>S. aureus</i>	Gram+ <i>S. epidermidis</i>	Gram+ <i>E. faecalis</i>	Gram+ <i>B. cereus</i>	Gram- <i>E. coli</i>	Gram- <i>P. aeruginosa</i>
GS	8	4	8	8	32	64
6	16	16	64	16	64	>64
7	16	8	64	16	64	>64
8	8	8	16	8	32	64
9	32	8	64	16	64	>64

The antibacterial assay indicated that none of the four analogs are significantly more potent than GS. Peptides **6** and **7** show decreased inhibitory activity for all Gram-positive bacteria tested, especially for *E. faecalis* as compared to GS. Compound **8** performs almost as well as GS, with the exception of the *E. faecalis* strain. Peptide **9** shows the same activity as **6** and **7**. As for the Gram-negative bacteria, GS does not show high antibacterial activity, and the same applies to the GS analogs. Peptides **6-9** were also evaluated for their toxicity towards mammalian membranes (Figure 7). All peptides are less hemolytic than GS, with **8** displaying hemolytic activity in the range of GS, and **6** being the least hemolytic.

Figure 7 Hemolytic activity of GA analogs **6-9**. Experiments were carried out in quadruplicate.

Conclusion

In this Chapter, four GS analogs were presented, in which one $^{\text{D}}$ Phe-Pro motif of the β -turn was replaced with morpholine amino acids. These analogs showed secondary structures similar to that of GS but with considerable differences in the MAA-

containing β -turn region. In Figure 9 of the Appendix, the β -turn structures of all compounds are summarized and compared to that of GS. Compound **8** shows the highest structural similarity with the natural product as judged by the $J_{\text{NH-H}\alpha}$ values, the chemical shifts of the α -protons and the NOE crosspeaks observed. Furthermore, a supramolecular structure is formed which shows remarkable resemblance to that of a SAA-containing GS analog published previously.^{11a} For GS analog **7**, it was observed from X-ray crystallography that one of the backbone amides ‘flips’ and as a consequence, only three hydrogen bonds can be formed between the backbone amides instead of the usual four hydrogen bonds. The distortion of the β -turn also reflects in the NMR data: large differences in chemical shift perturbations were observed. However, the NH-H α coupling constants do not show any differences. This distortion of the turn region has been observed as well in the SAA-containing GS analog mentioned above but for peptide **7**, no supramolecular structure is observed. Peptide **9** also differs from GS; in the NH region of the ¹H NMR spectrum peak broadening was observed, indicating conformational flexibility. Furthermore, the absence of certain NOE crosspeaks confirm the presence of a distorted β -turn.

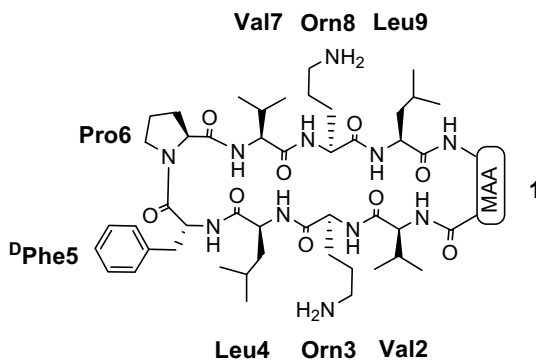
The analogs were also evaluated for their antibacterial and hemolytic activity. The peptides **6**, **7** and **9** displayed less hemolytic activity than GS, but unfortunately also displayed reduced antibacterial activity. This correlation between affinity for bacterial membranes and mammalian membranes has been reported before for other GS analogs, both modified in the β -turn and in the β -sheet^{2,11b,c,19} and could indicate a general trend. However, decrease in antibacterial activity does not always correlate to decrease in hemolytic activity. For example, peptide **6** contains a dipeptide isostere as replacement for the ^DPhe-Pro sequence and is structurally quite similar to GS, as judged by NMR analysis. It is the least hemolytic but does not show the lowest antibacterial activity. Compound **7**, which shows the ‘amide flip’, is somewhat more toxic than **6**, but shows the same activity against bacteria. Of this peptide series, only peptide **8** performed as well as GS. It also contains a dipeptide isostere, is from a structural point of view the best GS mimic, the most effective antibiotic, and shows the highest hemolytic activity in this series. However, this hemolytic activity is slightly decreased as compared to GS. Based on the NMR data, it is expected that peptide **9** will show a large distortion of the β -turn region. Although it is the least active compound against bacteria, it is not the least hemolytic. Interestingly, this peptide seems to show slight selectivity for the *S. epidermidis* and *B. cereus* strains, while less activity is seen for the other two Gram-positive bacteria. The same is the case for compound **7**. Apparently, replacement of the ^DPhe-Pro sequence with molecules larger than a dipeptide isostere is reasonably well tolerated. The spatial relationship between the carboxylic acid and the azidomethylene moieties (either *cis* or *trans*) does

have an influence on hemolytic activity, but no general trend can be observed. These results indicate that both antibacterial and hemolytic activity are influenced by changing the β -turn architecture, and also make clear that it is possible to modify GS in such a way that analogs are able to discriminate between bacterial and mammalian cells. GS itself does not possess these discriminatory properties. Furthermore, it can be concluded that MAA **4** is the best β -turn mimetic. Variation of the side chain of the dipeptide isostere **4** and replacement of one of the ^DPhe-Pro dipeptides with such a dipeptide isostere may provide GS analogs which retain their antibacterial activity, but are less hemolytic than GS.

Experimental Section

General

Reagents and solvents were used as provided, unless stated otherwise. THF was distilled over LiAlH_4 prior to use. Reactions were carried out under inert conditions and ambient temperature, unless stated otherwise. Prior to performing a reaction, traces of H_2O were removed from the starting materials by repeated coevaporation with anhydrous 1,4-dioxane, which was stored over 4 Å molsieves. Reactions were monitored by thin layer chromatography on aluminum coated silica sheets (Merck, silica 60 F₂₅₄), using visualization by spraying with a solution of 25 g $(\text{NH}_4)_2\text{MoO}_4$, 10 g $(\text{NH}_4)_4\text{Ce}(\text{SO}_4)_4$ in 100 ml H_2SO_4 and 900 ml H_2O , or a solution of 20% H_2SO_4 in ethanol, followed by charring at $\sim 150^\circ\text{C}$. Column chromatography was carried out with silica gel (Screening Devices bv, 40-63 μm particle size, 60 Å), using technical grade solvents. NMR spectra were recorded at 298K on a Bruker AV400 or a Bruker DMX600 using deuterated solvents. All carbon spectra are proton-decoupled. CD_3OH was used as provided, to CDCl_3 tetramethylsilane was added as an internal standard. Chemical shifts (δ) are given in ppm, in ^{13}C spectra relative to the solvent peaks of CDCl_3 (77.0 ppm) or CD_3OH (49.0 ppm), in ^1H spectra either relative to tetramethylsilane (0 ppm) or relative to the solvent peak of CD_3OH (3.31 ppm). Coupling constants are given in Hz. IR spectra were recorded on a Perkin Elmer Paragon 1000 FT-IR Spectrometer. High resolution mass spectra were recorded by direct injection (2 μL of a 2 μM solution in $\text{H}_2\text{O}/\text{MeCN}$; 50/50; v/v and 0.1% formic acid) on a mass spectrometer (Thermo Finnigan LTQ Orbitrap) equipped with an electrospray ion source in positive mode (source voltage 3.5 kV, sheath gas flow 10, capillary temperature 250°C) with resolution $R = 60000$ at m/z 400 (mass range $m/z = 150\text{--}2000$) and dioctylphthalate ($m/z = 391.28428$) as a “lock mass”. The high resolution mass spectrometer was calibrated prior to measurements with a calibration mixture (Thermo Finnigan). Optical rotations were measured on a Propol automatic polarimeter (sodium D-line, $\lambda = 589\text{ nm}$). Specific rotations (α_D) are given in degree per centimeter and the concentration c is given in grams per 100 ml in the specified solvent. Peptides were synthesized on solid support starting from pre-loaded Fmoc-Leu-HMPB-BHA resin (Novabiochem, 0.51 mmol g^{-1} , 100-200 Mesh) and amino acids were coupled manually using Fmoc based peptide synthesis methods and commercially available Fmoc amino acids. LC-MS analysis was performed on a Finnigan Surveyor HPLC system with a Gemini C₁₈ 50 \times 4.6 mm column (3 micron, Phenomenex, Torrance, CA, USA) (detection at 200-600 nm), coupled to a Thermo Finnigan LCQ Advantage Max mass spectrometer (Breda, The Netherlands) with electrospray ionization (ESI; system 1), in combination with buffers A: H_2O , B: MeCN and C: 1.0% aq. TFA. For RP-HPLC purification of the peptides, a BioCAD ‘Vision’ automated HPLC system (PerSeptiveBiosystems, inc.) supplied with a preparative Gemini C₁₈ column (Phenomenex, 150 \times 21.2 mm, 5 micron) was used. The applied buffers were A: H_2O , B: MeCN and C: 1.0% aq. TFA. For the assignment of all GS analogs, residue numbering was used as depicted on the right. All NMR signals were assigned as much as possible. Graphs were made using Graphpad Prism 5, and data concerning the hemolytic activity of the peptides were fitted using the same program.



Preparation of diazomethane

CAUTION: diazomethane is highly explosive, and therefore special precautions need to be taken during its preparation and use. All operations should be performed behind an explosion shield.

Furthermore, no mechanical stirring can be employed. Instead, mixing should take place by shaking the flask by hand. Finally, no metal utensils (like syringe needles) should be used.

To a thoroughly chilled mixture of 40% aq. KOH (13.5 ml) and Et₂O (37 ml) N-methyl-N-nitro-N-nitrosoguanidine (5.5 g, 37 mmol) was added in small portions. During the addition the solution was kept cold. After addition of the diazomethane precursor was complete, the thus generated diazomethane solution was added **in small portions** to the reaction mixture by taking a bit solution with a glass pipette, drying it over a few KOH pellets and then transferring it to the reaction flask, also using a glass pipette. Excess diazomethane solution should be quenched by carefully adding acetic acid to the chilled solution.

Antibacterial Assays

The following bacterial strains were used: *Staphylococcus aureus* (ATCC 29213), *Staphylococcus epidermidis* (ATCC 12228), *Enterococcus faecalis* (ATCC 29212), *Bacillus cereus* (ATCC 11778), *Escherichia coli* (ATCC 25922), *Pseudomonas aeruginosa* (ATCC 27853). Bacteria were stored at -70 °C and grown at 35 °C on Columbia Agar with sheep blood (Oxoid, Wesel, Germany) suspended in physiological saline until an optical density of 0.1 AU (at 595 nm, 1 cm cuvette). The suspension was diluted (100 x) with physiological saline, and 2 µl of this inoculum was added to 100 µl growth medium, Cation Adjusted Mueller Hinton II Broth (BBL ref. nr. 212322, lot nr. 7079753), in microtitre plates (96 wells). The peptides GS and **6-9** were dissolved in methanol (1 g/l) and two-fold diluted in the broth (64, 32, 16, 8, 4 and 1 mg/l). The plates were incubated at 35 °C (24 h) and the MIC was determined as the lowest concentration inhibiting bacterial growth.

Hemolytic assays

Freshly drawn heparinized blood was centrifuged for 10 minutes at 1000g at 10 °C. Subsequently, the erythrocyte pellet was washed three times with 0.85% saline solution and diluted with saline to a 1/25 packed volume of red blood cells. The peptides to be evaluated (**6-9** and GS) were dissolved in a 30% DMSO/0.5 mM saline solution to give a 1.5 mM solution of peptide. If a suspension was formed, the suspension was sonicated for a few seconds. A 1% Triton-X solution was prepared. Subsequently, 100 µl of saline solution was dispensed in columns 1-11 of a microtiter plate, and 100 µl of 1% Triton solution was dispensed in column 12. To wells A1-C1, 100 µl of the peptide was added and mixed properly. 100 µl of wells A1-C1 was dispensed into wells A2-C2. This process was repeated until wells A10-C10, followed by discarding 100 µl of wells A10-C10. These steps were repeated for the other peptides. Subsequently, 50 µl of the red blood cell suspension was added to the wells and the plates were incubated at 37 °C for 4 hours. After incubation, the plates were centrifuged at 1000g at 10 °C for 4 min. In a new microtitre plate, 50 µl of the supernatant of each well was dispensed into a corresponding well. The absorbance at 405 nm was measured and the percentage of hemolysis was determined.

Peptide Synthesis

a) Synthesis of resin-bound linear octamer (Scheme 2)

Peptide synthesis was performed using standard Fmoc SPPS methods. Elongation of the peptide chain was performed using repeating coupling cycles containing the following steps: i) Fmoc deprotection (20% piperidine/NMP, 15 min). ii) Peptide coupling (3 eq Fmoc-AA-OH, 3 eq HCTU, 3.6 eq DIPEA, NMP, 2h). For the synthesis of **6**, **8** and **9**, amino acids were attached in the following order, starting from pre-loaded Fmoc-Leu-HMPB-BHA resin: Fmoc-Orn(Boc)-OH, Fmoc-Val-OH, Fmoc-Pro-OH, Fmoc-^DPhe-OH, Fmoc-Leu-OH, Fmoc-Orn(Boc)-OH, Fmoc-Val-OH.

b) Attachment of MAA's, general procedure (Scheme 2)

The Fmoc group of the resin-bound octamer (150 µmol) was liberated using 20% piperidine/NMP. Subsequently, a solution of 2 eq MAA, 3 eq BOP, 3 eq HOBt and 3.5 eq DIPEA in NMP was added and the mixture shaken for 18 h. The coupling was monitored by Kaiserstest.

c) On-resin Staudinger reduction of the azide functionality, general procedure (Scheme 2)

After attachment of the MAA, the resin was washed thrice with 1,4-dioxane and suspended in 15 ml 1,4-dioxane. PMe_3 was added (as 1 M solution in toluene, 16 eq, 2.4 mmol, 2.4 ml) and the mixture shaken for two hours. H_2O was added (1.5 ml) and after another four hours, the resin was washed five times with 1,4-dioxane. The presence of the free amine was verified by Kaisertest.

d) Cleavage from resin, general procedure (Scheme 2)

The reduced peptide was cleaved from the resin (1% TFA/DCM, 4 x 10 min, 4 x 15 ml). The washings were collected in a toluene-containing flask (20 ml toluene) and concentrated to ~10% of the volume. This was done to prevent the mixture from becoming too acidic, with undesired cleavage of side chain protecting groups as a consequence. Fresh toluene was added and the solution again concentrated to 10% of the volume. Finally, another batch of toluene was added and the mixture concentrated to dryness to yield the crude peptide as a white solid.

d) Cyclization, general procedure (Scheme 2)

The linear peptide (150 μmol) was taken up in DMF (7.5 ml) and added dropwise during 1 h to a solution of PyBOP (0.39 g, 750 μmol , 5 eq), HOBt (0.10 g, 750 μmol , 5 eq) and DIPEA (0.39 ml, 2.25 mmol, 15 eq) in DMF (120 ml). After stirring overnight, the solvent was evaporated and the residue applied to a LH-20 size-exclusion column, using MeOH as eluent. The peptide was obtained as a yellowish solid.

e) Deprotection, general procedure (Scheme 2)

The crude protected peptide was dissolved in DCM (11 ml) and cooled to 0° C. TFA (11 ml) was added slowly and the mixture warmed to rt. After stirring for 30 min, solvents were evaporated and the residue coevaporated with toluene (three times) to remove all traces of TFA. The crude peptide was obtained as a yellowish solid and purified by RP-HPLC, using gradients of $\text{H}_2\text{O}/\text{MeCN}/1\%$ TFA. The fractions containing the pure product were pooled, concentrated and freeze-dried to yield the pure peptide.

Synthesis and analytical data of all compounds**3,7-Anhydro-5-aza-8-azido-5-benzyl-2,4,5,6,8-pentadeoxy-D-glycero-D-gluco-octonic acid (5)**

To a cooled (-25 °C) solution of diazoketone **10** (0.51 g, 1.69 mmol) in THF (17 ml) were added H_2O (1.7 ml) and silver trifluoroacetate (41 mg, 0.19 mmol) in Et_3N (0.68 ml, 4.9 mmol) under exclusion of light. The resulting mixture was warmed to rt over 3 h and stirred under exclusion of light. If TLC analysis did not show complete disappearance of starting material, the reaction was cooled again to -25 °C, 82 mg (0.37 mmol) of silver trifluoroacetate was added and the mixture warmed to rt in 3 h. This was repeated until completion of the reaction was seen on TLC. Et_2O and sat. aq. NaHCO_3 were added to the reaction and the layers were separated. The aqueous layer was extracted again with Et_2O and then acidified to pH = 5. After extracting 4 times with Et_2O , the combined organic layers were dried (Na_2SO_4), filtered and concentrated. The crude residue was purified by column chromatography (10 → 50% EtOAc/light petroleum) to yield pure **6** as a colorless oil (0.16 g, 0.56 mmol, 33%).

^1H NMR (CDCl_3 , 400 MHz): δ 10.46 (s, 1H, COOH); 7.36-7.23 (m, 5H, CH benzene ring); 4.42-4.26 (m, 1H, H_3); 4.04-3.98 (m, 1H, H_7); 3.59-3.48 (m, 3H, CH_2 benzyl, H_{8A}); 3.28 (dd, $J = 12.8$ Hz, $J = 4.9$ Hz, 1H, H_{8B}); 2.81 (dd, $J = 15.6$ Hz, $J = 7.4$ Hz, 1H, H_{2A}); 2.65 (dd, $J = 6.0$ Hz, $J = 15.4$ Hz, 1H, H_{2B}); 2.62 (dd, $J = 8.6$ Hz, $J = 2.8$ Hz, 1H, H_{4A}); 2.58 (dd, $J = 11.5$ Hz, $J = 3.0$ Hz, 1H, H_{6A}); 2.44 (dd, $J = 11.5$ Hz, $J = 5.1$ Hz, 1H, H_{4B}); 2.31 (dd, $J = 11.4$ Hz, $J = 6.6$ Hz, 1H, H_{6B}). ^{13}C NMR (CDCl_3 , 100 MHz): δ 175.9 (C=O acid); 136.4 (C_q benzene ring); 129.1 (CH benzene ring); 128.4 (CH benzene ring); 127.6 (CH benzene ring); 70.1 (C_7); 68.3 (C_3); 62.6 (CH_2 benzyl); 55.8 (C_4); 53.9 (C_6); 51.8 (C_8); 37.4 (C_2). IR (neat): 2929.8; 2812.0; 2363.7; 2342.9; 2096.4; 1717.7; 1559.9; 1457.4; 1399.8; 1362.7; 1272.8; 1108.3; 750.0; 698.8; 668.1. $[\alpha]_{\text{D}}^{20}$: +33.9 ($c = 0.79$, CHCl_3). LC-MS

retention time: 3.54 min (10 → 90% MeCN, 15 min run). Mass (ESI): m/z 291.07 [M + H]⁺. Exact mass: calculated for [C₁₄H₁₉N₄O₃]⁺: 291.14517. Found: 291.14536 [M + H]⁺.

Cyclo-(MAA-Val-Orn-Leu-^DPhe-Pro-Val-Orn-Leu).2TFA (6)

Following the general procedures for peptide synthesis and cleavage, **6** was obtained from **12** (loading 0.23 mmol g⁻¹, 652 mg, 150 μmol) as a white powder (56.5 mg, 31.6 μmol, 28%) using an HPLC gradient of 55:35:10 → 10:80:10 H₂O/MeCN/1% aq. TFA for purification.

¹H NMR (CD₃OH, 600 MHz): δ 8.98 (d, J = 3.2 Hz, 1H, NH ^DPhe₅); 8.71 (d, J = 8.8 Hz, 1H, NH Leu₄); 8.68 (d, J = 9.1 Hz, 1H, NH Orn₈); 8.61 (d, J = 8.8 Hz, 1H, NH Orn₃); 8.15 (d, J = 8.6 Hz, 1H, NH Leu₉); 8.09 (t, J = 5.9 Hz, 1H, NH MAA₁); 7.95 (s, 2H, NH Orn side chain); 7.92 (s, 2H, NH Orn side chain); 7.80 (d, J = 8.4 Hz, 1H, NH Val₇); 7.62 (d, J = 8.0 Hz, 1H, NH Val₂); 7.52-7.44 (m, 5H, CH benzene ring); 7.35-7.22 (m, 5H, CH benzene ring); 4.77-4.72 (m, 1H, H_α Orn₈); 4.65 (dd, J = 15.8 Hz, J = 7.3 Hz, 1H, H_α Leu₄); 4.58-4.49 (m, 2H, H_α Leu₉, ^DPhe₅); 4.44 (d, J = 10.8 Hz, 1H, H₂ MAA₁); 4.39-4.29 (m, 3H, H_α Val₂, Orn₃, Pro₆); 4.06 (t, J = 8.9 Hz, 1H, H_α Val₇); 4.04-4.00 (m, 1H, H₆ MAA₁); 3.76-3.71 (m, 1H, H_{δA} Pro₆); 3.65 (s, 2H, CH₂ benzyl MAA₁); 3.59-3.54 (m, 1H, H_{7A} MAA₁); 3.41-3.32 (m, 1H, H_{7B} MAA₁); 3.09 (dd, J = 12.6 Hz, J = 5.0 Hz, 1H, H_{βA} ^DPhe₅); 2.95-2.92 (m, 5H, H_{βB} ^DPhe, H_δ Orn₃, Orn₈); 2.81 (q, J = 21.8 Hz, J = 11.0 Hz, 4H, H₅ and H₃ MAA₁); 2.49 (dd, J = 17.3 Hz, J = 8.7 Hz, 1H, H_{βB} Pro₆); 2.33-2.25 (m, 1H, H_β Val₇); 2.15-2.08 (m, 1H, H_β Val₂); 2.05-1.91 (m, 2H, H_β Pro₆); 1.88-1.42 (m, 12H, H_γ Pro₆, H_β Leu₄, Leu₉, H_γ Leu₄, Leu₉, H_β Orn₃, Orn₈); 0.92-0.87 (m, 24H, H_γ Val₂, Val₇, H_δ Leu₄, Leu₉). ¹³C NMR (CD₃OH, 150 MHz): δ 174.7 (C=O amide); 173.7 (C=O amide); 173.5 (C=O amide); 173.3 (C=O amide); 172.9 (C=O amide); 172.6 (C=O amide); 171.8 (C=O amide); 168.7 (C=O amide); 136.9 (C_q benzene ring); 132.2 (CH benzene ring); 131.1 (CH benzene ring); 130.6 (C_q benzene ring); 130.4 (CH benzene ring); 130.3 (CH benzene ring); 130.2 (CH benzene ring); 129.7 (CH benzene ring); 128.5 (CH benzene ring); 73.6 (C₆ MAA₁); 73.4 (C₂ MAA₁); 61.9 (C_α Pro₆); 60.9 (C_α Val₇); 58.8 (C_α Orn₃, Val₂); 55.9 (C_α ^DPhe₅); 53.6 (C_α Orn₈); 53.6 (C₅ MAA₁); 53.2 (C_α Leu₉); 52.9 (C₃ MAA₁); 51.7 (C_α Leu₄); 47.9 (C₈); 42.3; 42.1 (C_β Leu₄, Leu₉); 41.3 (C₇ MAA₁); 40.8; 40.7 (C₈ Orn₃, Orn₈); 37.3 (C_β ^DPhe₅); 33.4 (C_β Val₂); 31.5 (C_β Val₇); 30.5; 30.2; 30.0 (C_β Pro₆, C_γ Orn₃, Orn₈); 26.0; 25.7 (C_γ Leu₄, Leu₉); 25.0; 24.9; 24.5 (C_γ Pro₆, C_β Orn₃, Orn₈); 23.4; 23.1; 23.0; 21.9; 19.8; 19.4; 18.6 (C_γ Val₂, Val₇, C₈ Leu₄, Leu₉). IR (neat): 2926.1; 2191.9; 2153.0; 2002.3; 1668.0; 1635.1; 1538.0; 1455.7; 1201.5; 1133.9; 832.3; 799.4; 753.6; 721.4; 702.1; 667.9. LC-MS retention time: 6.82 min (10 → 90% MeCN, 15 min run). Mass (ESI): m/z 565.47 [M + 2H]²⁺; 1129.73 [M + H]⁺. Exact mass: calculated for [C₅₉H₉₄N₁₂O₁₀]²⁺: 565.36025; [C₅₉H₉₃N₁₂O₁₀]⁺: 1129.71321. Found: 565.35996 [M + 2H]²⁺; 1129.71411 [M + H]⁺.

Cyclo-(MAA-Val-Orn-Leu-^DPhe-Pro-Val-Orn-Leu).2TFA (7)

Following the general procedures for peptide synthesis and cleavage, **7** was obtained from **12** (loading 0.23 mmol g⁻¹, 207 mg, 48 μmol) as a white powder (46.3 mg, 31.7 μmol, 66%) using an HPLC gradient of 55:35:10 → 10:80:10 H₂O/MeCN/1% aq. TFA for purification.

Analytical data corresponded to those reported.¹³

Cyclo-(MAA-Val-Orn-Leu-^DPhe-Pro-Val-Orn-Leu).2TFA (8)

Following the general procedures for peptide synthesis and cleavage, **8** was obtained from **12** (loading 0.23 mmol g⁻¹, 652 mg, 150 μmol) as a white powder (63.9 mg, 47.1 μmol, 31%) using an HPLC gradient of 60:30:10 → 20:70:10 H₂O/MeCN/1% aq. TFA for purification.

¹H NMR (CD₃OH, 600 MHz): δ 8.97 (d, J = 3.2 Hz, 1H, NH ^DPhe₅); 8.78 (d, J = 9.3 Hz, 1H, NH Orn₃); 8.71 (d, J = 9.1 Hz, 1H, NH Leu₄); 8.70 (d, J = 9.0 Hz, 1H, NH Orn₈); 8.34 (d, J = 9.5 Hz, 1H, NH Leu₉); 8.27 (br s, 1H, NH MAA₁); 7.88 (s, 2H, NH Orn side chain); 7.78 (d, J = 8.7 Hz, 3H, NH Val₇, NH Orn side chain); 7.52-7.43 (m, 5H, CH benzene ring); 7.34-7.22 (m, 5H, CH benzene ring); 7.10 (d, J = 7.7 Hz, 1H, αNH Val₂); 5.03 (dt, J = 9.2 Hz, J = 6.2 Hz, 1H, H_α Orn₈); 4.73-4.63 (m, 3H, H_α Orn₃, Leu₉, Leu₄); 4.52-4.47 (m, 1H, H_α ^DPhe); 4.40 (dd, J = 8.3 Hz, J = 5.2 Hz, 1H, H_α Val₂); 4.36-4.23 (m, 1H, H_α Pro₆); 4.18-4.12 (m, 1H, H₂ MAA₁); 4.02 (t, J = 9.0 Hz, 1H, H_α Val₇); 3.73 (t, J = 7.9 Hz, 1H, H_{δA} Pro₆); 3.65 (s, 2H, CH₂ benzyl MAA₁); 3.51 (d, J = 11.0 Hz,

1H, H₆ MAA₁); 3.27 (s, 2H, H₃ MAA₁); 3.16-3.11 (m, 1H, H_{7A} MAA₁); 3.09 (dd, $J = 12.6$ Hz, $J = 4.9$ Hz, 1H, H_{βA} ^DPhe₅); 3.06-2.84 (m, 8H, H_δ Orn₃, Orn₈, H_{βB} ^DPhe₅, H₅ MAA₁, H_{7B} MAA₁); 2.46 (q, $J = 9.4$ Hz, $J = 9.3$ Hz, 1H, H_{δB} Pro₆); 2.34-2.24 (m, 1H, H_β Val₇); 2.08-1.95 (m, 3H, H_β Val₂, H_β Orn₈); 1.94-1.87 (m, 1H, H_{βA} Orn₃); 1.81-1.61 (m, 12H, H_γ Orn₃, Orn₈, H_{γA} Pro₆, H_β Pro₆, H_{βB} Orn₃, H_β Leu, H_γ Leu); 1.60-1.48 (m, 3H, H_{βA} Leu, H_{γB} Pro₆, H_γ Leu); 1.45-1.37 (m, 1H, H_{βB} Leu); 0.96 (d, $J = 6.63$ Hz, 3H, H_γ Val₇); 0.92-0.85 (m, 21H, H_γ Val₂, Val₇, H_δ Leu₄, Leu₉). ¹³C NMR (CD₃OH, 150 MHz): δ 175.3 (C=O amide); 173.7 (C=O amide); 173.5 (C=O amide); 173.1 (C=O amide); 172.8 (C=O amide); 172.7 (C=O amide); 171.6 (C=O amide); 169.3 (C=O amide); 136.9 (C_q benzene ring); 132.4 (CH benzene ring); 131.1 (CH benzene ring); 130.4 (CH benzene ring); 130.2 (CH benzene ring); 129.7 (CH benzene ring); 128.5 (CH benzene ring); 73.4 (C₂ MAA₁); 68.1 (CH₂ benzyl MAA₁); 62.9; 61.9 (C_α Pro₆); 61.0 (C_α Val₇); 58.4 (C_α Val₂); 56.0 (C_α ^DPhe₅); 53.5 (C_α Orn₃); 52.8 (C_α Orn₈); 52.1 (C₃ MAA₁); 51.9 (C_α Leu₉, C₆ MAA₁); 51.6 (C_α Leu₄); 47.9 (C₈ Pro₆); 47.3 (C₇ MAA₁); 42.5; 42.1 (C_β Leu₄, Leu₉); 40.6; 40.5; 40.4 (C_δ Orn₃, Orn₈, C₅ MAA₁); 37.3 (C_β ^DPhe); 33.6 (C_β Val₂); 31.5 (C_β Val₇); 30.6; 30.4; 29.8 (C_β Orn₃, Orn₈, C_γ Pro₆); 25.9; 25.7 (C_γ Leu₄, Leu₉); 25.0; 24.8; 24.4 (C_γ Orn₃, Orn₈, C_β Pro₆); 24.1; 23.1; 21.3; 19.7; 19.7; 19.4; 18.3 (C_γ Val₂, Val₇, C₈ Leu₄, Leu₉). IR (neat): 3294.1; 2963.7; 2169.5; 2153.8; 2003.9; 1978.1; 1966.5; 1657.1; 1651.6; 1634.2; 1563.0; 1557.7; 1531.9; 1505.8; 1455.7; 1200.3; 1130.4; 835.9; 799.2; 749.2; 721.6; 702.1; 667.9; 589.6; 505.5. LC-MS retention time: 6.96 min (10 → 90% MeCN, 15 min run). Mass (ESI): m/z 565.47 [M + 2H]²⁺; 1129.60 [M + H]⁺. Exact mass: calculated for [C₅₉H₉₄N₁₂O₁₀]²⁺: 565.36025; [C₅₉H₉₃N₁₂O₁₀]⁺: 1129.71321. Found: 565.35986 [M + 2H]²⁺; 1129.71397 [M + H]⁺.

Cyclo-(MAA-Val-Orn-Leu-^DPhe-Pro-Val-Orn-Leu).2TFA (9)

Following the general procedures for peptide synthesis and cleavage, **9** was obtained from **12** (loading 0.23 mmol g⁻¹, 652 mg, 150 μmol) as a white powder (105.5 mg, 76.9 μmol, 52%) using an HPLC gradient of 60:30:10 → 35:55:10 H₂O/MeCN/1% aq. TFA for purification.

¹H NMR (CD₃OH, 600 MHz): δ 8.93 (d, $J = 3.2$ Hz, 1H, NH ^DPhe); 8.70 (d, $J = 8.5$ Hz, 1H, NH Orn); 8.63 (d, $J = 8.9$ Hz, 1H, NH Leu); 8.45 (s, 1H, NH Leu); 8.38 (d, $J = 8.9$ Hz, 1H, NH Orn); 8.00 (s, 1H, NH Val); 7.84 (br s, NH Orn side chains); 7.79 (d, $J = 8.5$ Hz, 1H, NH Val); 7.49-7.45 (m, 2H, CH benzene ring); 7.44-7.42 (m, 3H, CH benzene ring); 7.33-7.23 (m, 5H, CH benzene ring); ~4.9 (H_α Orn, not visible due to solvent suppression); 4.62 (q, $J = 7.8$ Hz, $J = 7.6$ Hz, 1H, H_α Leu); 4.57-4.48 (m, 2H, H_α Orn, ^DPhe); 4.39 (ddd, $J = 11.4$ Hz, $J = 8.2$ Hz, $J = 3.4$ Hz, 1H, H_α Leu); 4.34 (d, $J = 6.5$ Hz, 1H, H_α Pro); 4.20-4.15 (m, 1H, H MAA); 4.13 (s, 1H, H MAA); 3.99 (t, $J = 8.9$ Hz, 1H, H_α Val); 3.96-3.93 (m, 1H, H_α Val); 3.72 (t, $J = 7.5$ Hz, 1H, H_{δA} Pro); 3.65 (s, 2H, CH₂ benzyl MAA₁); 3.49 (s, 1H, MAA); 3.20 (d, $J = 10.1$ Hz, 1H, MAA); 3.11 (s, 1H, MAA); 3.08 (dd, $J = 12.6$ Hz, $J = 5.1$ Hz, 1H, H_{βA} ^DPhe); 3.04-2.91 (m, 8H, H_{βB} ^DPhe, H_δ Orn, MAA); 2.50 (q, $J = 9.2$ Hz, $J = 9.1$ Hz, 1H, H_{δB} Pro); 2.30-2.23 (m, 1H, H_β Val); 2.01 (dd, $J = 14.1$ Hz, $J = 7.2$ Hz, 1H, H_β Val); 1.89-1.83 (m, 1H, H_{βA} Orn); 1.78-1.71 (m, 4H, H_γ Orn, H_β Orn); 1.71-1.64 (m, 5H, H_{βB} Pro, H_{βB} Orn, H_{γA} Pro, H_γ Orn); 1.62-1.49 (m, 6H, H_{γB} Pro, H_{βA} Leu, H_γ Leu, H_β Leu); 1.43 (dd, $J = 13.0$ Hz, $J = 6.7$ Hz, 1H, H_{βB} Leu); 1.02 (d, $J = 6.6$ Hz, 3H, H_γ Val); 0.95 (dd, $J = 6.6$ Hz, $J = 2.1$ Hz, 6H, H_γ Val); 0.92 (d, $J = 6.5$ Hz, 3H, H_δ Leu); 0.90 (d, $J = 6.4$ Hz, 3H, H_δ Leu); 0.87 (d, $J = 6.4$ Hz, 6H, H_γ Val, H_δ Leu); 0.84 (s, $J = 6.3$ Hz, 3H, H_δ Leu). ¹³C NMR (CD₃OH, 150 MHz): δ 175.2 (C=O amide); 173.8 (C=O amide); 173.7 (C=O amide); 173.4 (C=O amide); 173.2 (C=O amide); 173.1 (C=O amide); 172.8 (C=O amide); 136.9 (C_q benzene ring); 132.0 (CH benzene ring); 130.4 (CH benzene ring); 130.0 (CH benzene ring); 129.7 (CH benzene ring); 128.5 (CH benzene ring); ~69.0 (MAA) 68.1 (CH₂ benzyl MAA); 63.0 (MAA); 61.8 (C_α Pro, Val); 61.0 (C_α Val); 55.8 (C_α ^DPhe); 55.5 (MAA); 53.9 (C_α Orn); 53.8 (C_α Leu, MAA); 53.1 (C_α Orn); 51.8 (C_α Leu); 47.9 (C₈ Pro); 42.4 (C_β Leu); 41.0; 41.0; 40.9; 40.8; 40.7 (C_δ Orn, C_β Leu, MAA); 37.4 (C_β ^DPhe); 31.7 (C_β Val); 31.2 (C_β Val); 30.7; 30.6; 29.5 (C_β Orn, C_β Pro); 26.0; 25.8 (C_γ Leu); 25.1; 24.7; 24.5 (C_γ Orn, C_γ Pro); 23.7; 23.1; 23.0; 21.4 (C_δ Leu); 19.8; 19.7; 19.5; 19.5 (C_γ Val). IR (neat): 3276.0; 2964.3; 1674.0; 1668.1; 1661.6; 1657.7; 1651.8; 1644.3; 1639.8; 1634.4; 1557.7; 1553.2; 1543.7; 1538.2; 1520.6; 1455.8; 1201.3; 1181.1; 1131.0; 836.7; 799.7; 721.9; 702.1; 668.0; 507.7. LC-MS retention time: 6.82 min (10 → 90% MeCN, 15 min run). Mass (ESI): m/z 572.47 [M + 2H]²⁺; 1143.80 [M + H]⁺. Exact

mass: calculated for $[C_{60}H_{96}N_{12}O_{10}]^{2+}$: 572.36807; $[C_{60}H_{95}N_{12}O_{10}]^+$: 1143.72886. Found: 572.36773 $[M + H]^+$; 1143.73019 $[M + H]^{2+}$.

3,7-Anhydro-5-aza-8-azido-5-benzyl-1-diazo-2,4,5,6,8-pentadeoxy-D-glycero-D-gluco-octon-2-one (10)

A solution of morpholine **4** (0.88 g, 3.17 mmol) in THF (16 ml) was cooled to $-15\text{ }^{\circ}\text{C}$. Et_3N (0.44 ml, 3.17 mmol) and ethyl chloroformate (0.30 ml, 3.17 mmol) were added and the mixture stirred for 15 min and then warmed slowly to $0\text{ }^{\circ}\text{C}$. A freshly prepared diazomethane solution (see general procedures) was added in small portions until the bright yellow color persisted. After slowly warming the reaction mixture to rt and stirring for 3 h, AcOH was added dropwise to quench the excess diazomethane. After washing with sat. aq. NaHCO_3 , sat. aq. NH_4Cl and sat. aq. NaCl, the combined aqueous layers were backextracted with Et_2O and the combined organic layers dried (Na_2SO_4), filtered and concentrated. The resulting brown oil was purified by column chromatography ($0 \rightarrow 20\%$ EtOAc/light petroleum) and pure **10** was obtained as a bright yellow oil (0.51 g, 1.69 mmol, 53%).

^1H NMR (CDCl_3 , 400 MHz): δ 7.33-7.22 (m, 5H, CH benzene ring); 5.83 (s, 1H, H_1); 4.27 (t, $J = 4.1$ Hz, 3H, H_3); 4.00 (qd, $J = 11.0$ Hz, $J = 3.6$ Hz, $J = 3.6$ Hz, 1H, H_7); 3.56-3.43 (m, 3H, CH_2 benzyl, H_{8A}); 3.23 (dd, $J = 13.0$ Hz, $J = 4.1$ Hz, 1H, H_{8B}); 2.96 (dd, $J = 11.5$ Hz, $J = 4.7$ Hz, 1H, H_{4A}); 2.56 (dd, $J = 11.5$ Hz, $J = 3.9$ Hz, 1H, H_{4B}); 2.48 (dd, $J = 11.5$ Hz, $J = 2.7$ Hz, 1H, H_{6A}); 2.18 (dd, $J = 11.4$ Hz, $J = 7.1$ Hz, 1H, H_{6B}). ^{13}C NMR (CDCl_3 , 100 MHz): δ 193.6 (C=O); 136.9 (C_q benzene ring); 128.9 (CH benzene ring); 128.3 (CH benzene ring); 127.3 (CH benzene ring); 76.2 (C_7); 72.3 (C_3); 62.7 (CH_2 benzyl); 53.7 (C_4); 53.2 (C_1); 52.8 (C_6); 51.9 (C_8). LC-MS retention time: 3.96 min ($10 \rightarrow 90\%$ MeCN, 15 min run). Mass (ESI): m/z 301.00 $[M + H]^+$.

References

1. Gause, G. F.; Brazhnikova, M. G. *Nature* **1944**, *154*, 703.
2. Kondejewski, L. H.; Farmer, S. W.; Wishart, D. S.; Hancock, R. E. W.; Hodges, R. S. *Int. J. Peptide Protein Res.* **1996**, *47*, 460-466.
3. Schmidt, G. M. J.; Hodgkin, D. C.; Oughton, B. M. *Biochem. J.* **1957**, *65*, 744-750.
4. Prenner, E. J.; Lewis, R. N. A. H.; McElhaney, R. N. *Biochim. Biophys. Acta* **1999**, *1462*, 201-221.
5. a) Stern, A.; Gibbons, W. A.; Craig, L. C. *Proc. Natl. Acad. Sci. USA* **1968**, *61*, 734-741. b) Hull, S. E.; Karlsson, R.; Main, P.; Woolfson, M. M.; Dobson, E. J. *Nature* **1978**, *275*, 206-207. c) Liquori, A.; De Santis, P. *Int. J. Biol. Macromol.* **1980**, *2*, 112-115. d) Rackovsky, S.; Scheraga, H. A. *Proc. Natl. Acad. Sci. USA* **1980**, *77*, 6965-6967.
6. O' Grady, F.; Greenwood, D. in *Antibiotic and chemotherapy: anti-infective agents and their use in therapy*; ed. O' Grady, F. (Churchill Livingstone, New York); **1997**, pp 337-338.
7. a) Hancock, R. E. W. *Lancet Infect. Dis.* **2001**, *1*, 156-164. b) Marr, A. K.; Gooderham, W. J.; Hancock, R. E. W. *Curr. Opin. Pharmacol.* **2006**, *6*, 468-472.
8. a) Sato, K.; Nagai, U. *J. Chem. Soc. Perkin Trans. 1* **1986**, 1231-1234. b) Bach, A. C.; Markwalder, J. A.; Ripka, W. C. *Int. J. Peptide Protein Res.* **1991**, *38*, 314-323.

9. Roy, S.; Lombart, H. G.; Lubell, W. D.; Hancock, R. E. W.; Farmer, S. W. *J. Pep. Res.* **2002**, *60*, 198-214.
10. a) De la Figuera, N.; Alkorta, I.; Garcia-Lopez, M. T.; Herranz, R.; Gonzalez-Muniz, R. *Tetrahedron* **1995**, *51*, 7841-7856. b) Ripka, W. C.; De Lucca, G. V.; Bach, A. C.; Pottorf, R. S.; Blaney, J. M. *Tetrahedron* **1993**, *49*, 3609-3628.
11. a) Grotenbreg, G. M.; Timmer, M. S. M.; Llamas-Saiz, A. L.; Verdoes, M.; Van der Marel, G. A.; Van Raaij, M. J.; Overkleeft, H. S.; Overhand, M. *J. Am. Chem. Soc.* **2004**, *126*, 3444-3446. b) Grotenbreg, G. M.; Kronemeijer, M.; Timmer, M. S. M.; El Oualid, F.; Van Well, R. M.; Verdoes, M.; Spalburg, E.; Van Hooft, P. A. V.; De Neeling, A. J.; Noort, D.; Van Boom, J. H.; Van der Marel, G. A.; Overkleeft, H. S.; Overhand, M. *J. Org. Chem.* **2004**, *69*, 7851-7859. c) Grotenbreg, G. M.; Buizert, A. E. M.; Llamas-Saiz, A. L.; Spalburg, E.; Van Hooft, P. A. V.; De Neeling, A. J.; Noort, D.; Van Raaij, M. J.; Van der Marel, G. A.; Overkleeft, H. S.; Overhand, M. *J. Am. Chem. Soc.* **2006**, *128*, 7559-7565.
12. Wijtman, R.; Vink, M. K. S.; Schoemaker, H. E.; Van Delft, F. L.; Blaauw, R. H.; Rutjes, F. P. J. T. *Synthesis* **2004**, 641-662.
13. Grotenbreg, G. M.; Christina, A. E.; Buizert, A. E. M.; Van der Marel, G. A.; Overkleeft, H. S.; Overhand, M. *J. Org. Chem.* **2004**, *69*, 8331-8339.
14. Podlech, J.; Seebach, D. *Liebigs Ann.* **1995**, 1217-1228.
15. Wüthrich, K. in *NMR of proteins and nucleic acids*; ed. John Wiley & Sons (Wiley-Interscience; New York); **1986**, pp 162-175.
16. Wishart, D. S.; Sykes, B. D.; Richards, F. M.; *Biochemistry* **1992**, *31*, 1647-1651.
17. Aravinda, S.; Harini, V. V.; Shamala, N.; Das, C.; Balaram, P. *Biochem.* **2004**, *43*, 1832-1846.
18. Llamas-Saiz, A. L.; Grotenbreg, G. M.; Overhand, M.; Van Raaij, M. J. *Acta Cryst.* **2007**, *D63*, 401-407.
19. a) Kondejewski, L. H.; Jelokhani-Niaraki, M.; Farmer, S. W.; Lix, B.; Kay, C. M.; Sykes, B. D.; Hancock, R. E. W.; Hodges, R. S. *J. Biol. Chem.* **1999**, *274*, 13181-13192. b) Jelokhani-Niaraki, M.; Kondejewski, L. H.; Farmer, S. W.; Hancock, R. E. W.; Kay, C. M.; Hodges, R. S. *Biochem. J.* **2000**, *349*, 747-755. c) Kawai, M.; Yamamura, H.; Tanaka, R.; Umemoto, H.; Ohmizo, C.; Higuchi, S.; Katsu, T. *J. Peptide Res.* **2005**, *65*, 98-104. d) Jelokhani-Niaraki, M.; Hodges, R. S.; Meissner, J. E.; Hassenstein, U. E.; Wheaton, L. *Biophys. J.* **2008**, *95*, 3306-3321. e) Solanas, C.; De la Torre, B. G.; Fernández-Reyes, M.; Santiveri, C. M.; Jiménez, M. A.; Rivas, L.; Jiménez, A. I.; Andreu, D.; Cativiela, C. *J. Med. Chem.* **2009**, *52*, 664-674.